Materials Characterization 155 (2019) 109819

Contents lists available at ScienceDirect

Materials Characterization

journal homepage: www.elsevier.com/locate/matchar

Microstructure and mechanical behaviour of aluminium-carbon steel and aluminium-stainless steel clads produced with an aluminium interlayer

G.H.S.F.L. Carvalho[a], I. Galvão[a,b], R. Mendes[c], R.M. Leal[a,d,*], A. Loureiro[a]

[a] CEMMPRE, Department of Mechanical Engineering, University of Coimbra, Portugal
[b] ISEL, Department of Mechanical Engineering, Polytechnic Institute of Lisbon, Portugal
[c] ADAI, LEDAP, Department of Mechanical Engineering, University of Coimbra, Portugal
[d] LIDA-ESAD.CR, Polytechnic Institute of Leiria, Portugal

ARTICLE INFO

Keywords:
Explosive welding
Weldability
Solid-state processes
Dissimilar welding
Intermetallic phases
Interlayer

ABSTRACT

The influence of an interlayer on the microstructure and the mechanical behaviour of aluminium-carbon steel and aluminium-stainless steel clads produced by explosive welding was studied. Different series of welds were produced both with and without an aluminium interlayer, testing different welding parameters. The combination of aluminium to carbon steel presented a better weldability than aluminium to stainless steel. For both couples, low-velocity welds presented the best microstructure and mechanical strength. The mechanical tests showed that the aluminium to carbon steel joining did not benefit from the use of the interlayer. A joint with good interfacial morphology and excellent tensile-shear properties was achieved by low-velocity direct welding, with the fracture occurring outside the joining region. For the aluminium to stainless steel couple, the use of the interlayer increased its weldability. However, the mechanical strength of the joint is restricted by the low strength of the interlayer. The presence of intermetallic compounds at the weld interface, does not, by itself, promote the poor-quality of the explosive weld. The way the interface accommodates and distributes these intermetallics dictates the weld's quality.

1. Introduction

The impact welding processes present a great potential for joining materials with very different physical properties and an easy formation of intermetallic phases. Although high peak temperatures are locally reached in impact welding, these processes present quite a short cycle time, minimising the interaction of the welded materials under high temperature. One of the main focuses of impact welding research has been the dissimilar joining of aluminium (Al) and ferrous alloys, specifically, carbon steel (CS) and stainless steel (SS). These combinations are of a very high technical interest due to enabling the combination of the low density (light-weight components) and the excellent thermal and electrical properties of the aluminium alloys with the low cost and the strength of carbon steel or the high corrosion resistance of stainless steels in a single component or structure. A proof of the scientific relevance of aluminium-steel joining by impact welding is the recent increase in the works published in this field, such as the studies undertaken by Carvalho et al. [1] in explosive welding of carbon steel and aluminium; Geng et al. [2] in magnetic pulse welding of aluminium and low alloy steel; Su et al. [3] in vaporising foil actuator welding of aluminium and low alloy steel; and Wang et al. [4] in laser shock welding of aluminium and stainless steel.

Among these processes, explosive welding is the most appropriate process for the production of large clads [5], and is therefore of great interest to many sectors for which the aluminium-carbon steel (Al-CS) and aluminium-stainless steel (Al-SS) joining are especially relevant, such as shipbuilding [6–8], automotive construction [9] or energy [10] industries. Each application has its particularities and requirements (such as corrosion resistance, fatigue, toughness), and authors like Kaya [6] and Corigliano et al. [11] presented relevant contributions regarding the welding of aluminium with ferrous alloys, proving the suitability of the explosive welding process for applications for aluminium to steel joints. However, as studied by Carvalho et al. [1,12], if thick and continuous intermetallic layers are formed at the interface of Al-CS and Al-SS explosive welds, welding failure tends to occur. Carvalho et al. [1] reported that this effect is mostly related to the physical properties of the intermetallic phases. These researches pointed also highlighted the detrimental effect of high collision point and impact velocities on the joining of both combinations.

The Al-CS and Al-SS welding conditions can be improved by

* Corresponding author at: CEMMPRE, Department of Mechanical Engineering, University of Coimbra, Portugal.
E-mail address: rui.leal@dem.uc.pt (R.M. Leal).

https://doi.org/10.1016/j.matchar.2019.109819
Received 26 April 2019; Received in revised form 8 July 2019; Accepted 15 July 2019
Available online 16 July 2019
1044-5803/

Table 1
Welding parameters.

	Weld series							
	A.304-L	A.I.304-L	A.304-H	A.I.304-H	A.CS-L	A.I.CS-L	A.CS-H	A.I.CS-H
Flyer plate	AA6082	AA6082	AA6082	AA6082	AA6082	AA6082	AA6082	AA6082
Baseplate	AISI 304	AISI 304	AISI 304	AISI 304	EN10130	EN10130	EN10130	EN10130
Interlayer	–	AA1050	–	AA1050	–	AA1050	–	AA1050
Expl. mixture	ANFO	ANFO	E + EPS	E + EPS	ANFO	ANFO	E + EPS	E + EPS
R	2.5	2.5	1	1	2.5	2.5	1	1

decreasing the detonation velocity (V_d) of the explosive mixture (and consequently the collision point velocity (V_c)) or the impact velocity of the flyer plate. As decreasing the detonation velocity below a certain value is especially difficult, the most straightforward strategy consists in decreasing the impact velocity (V_p), which can be achieved by inserting an intermediate plate between the flyer and the baseplate, i.e. an interlayer [13]. This way, the flyer will first collide with the interlayer, losing velocity and kinetic energy before finally colliding with the baseplate. This strategy has been tested for some combinations, such as titanium alloys and stainless steel [14], titanium alloys and low-alloy steel [15], titanium and magnesium alloys [16], titanium and aluminium alloys [17], and aluminium and copper alloys [18].

Regarding the combination of aluminium and ferrous alloys, this issue has been explored in only a few studies. Hokamoto et al. [19], on the explosive welding of four different aluminium alloys (AA1100, AA5083, AA2017, AA7075) to 304 stainless steel, reported that the thickness of the intermetallic layer formed at the weld interface could be decreased by welding with a stainless-steel interlayer. In turn, Han et al. [20], concerning explosive welding of aluminium to carbon steel, reported that consistent welds were achieved only when an AA1050 interlayer was used. These authors concluded that the increase in the thickness of the interlayer promotes a decrease in the weld strength. More recently, Aceves et al. [21], related to the explosive welding of aluminium to stainless steel, studied the insertion of two interlayers in the joint, i.e. a soft aluminium interlayer and a dissimilar interlayer. Three different materials were tested for the dissimilar interlayer: titanium, tantalum, and copper alloys. According to these authors, the highest weld strength was obtained with a titanium interlayer, while a tantalum interlayer led to maximum ductility. Worse results were achieved with a copper interlayer due to the formation of brittle intermetallic phases at the weld interface.

Although Al-CS and Al-SS explosive welding with an interlayer has been studied in a few previous works, the analysis of the microstructural phenomena occurring at the interface and its effect on the mechanical behaviour of the welds still requires more extensive research. Moreover, studies relating the weldability of different aluminium-ferrous alloy combinations to the effectiveness of welding with an interlayer are very incipient. The comparison of the microstructure, intermetallic formations and mechanical behaviour makes for a better understanding of the phenomena occurring at the interface of these welded combinations. So, the present research aims to study the influence of the interlayer on the microstructure and the mechanical behaviour of Al-CS and Al-SS clads produced by explosive welding. Different series of welds were produced with and without an interlayer, testing different welding parameters. In order to characterise the microstructural and the mechanical properties of the welds in depth, a broad range of techniques were used, such as optical microscopy, scanning electron microscopy (SEM), energy dispersive X-ray spectroscopy (EDS), electron backscattering diffraction (EBSD), nanoindentations, and tensile-shear testing.

2. Materials and methods

Aluminium-carbon steel and aluminium-stainless steel clads were manufactured by explosive welding. The base materials were 3 mm-thick plates of AA6082-T6, EN10130 (DC06) carbon steel, and AISI 304 stainless steel, with a hardness of 114 $HV_{0.2}$, 99 $HV_{0.2}$, and 181 $HV_{0.2}$, respectively. Four weld series were produced for each welded combination. Two series were produced by direct welding (without an interlayer), and two series were produced with an interlayer. The interlayer was a 1 mm-thick plate of AA1050, with a hardness of 40 $HV_{0.2}$. The 6082 aluminium alloy was the flyer plate in all welds, while the ferrous alloys were the stationary baseplate. All the welds were produced in a parallel full overlap joint configuration.

Regarding the explosives, two mixtures with different detonation velocities were tested: an explosive mixture with a lower detonation velocity (ANFO), and an explosive mixture with a higher detonation velocity (emulsion-based mixture sensitised with expanded polystyrene spheres: E + EPS) [22]. Two values of explosive ratio (R), which is the ratio between the explosive mixture and the flyer masses, were used. The explosive ratio of the welds produced with ANFO was 2.5, while the explosive ratio of the welds produced with E + EPS was 1. The stand-off distance (STD) was kept constant for each welding configuration. The direct welding was conducted with an STD of 4.5 mm, while two STDs were defined in the welds produced with an interlayer: the distance between the flyer plate and the interlayer was 4.5 mm, and the distance between the interlayer and the baseplate was 1.5 mm. The welding parameters used to produce the welds are summarised in Table 1.

The nomenclature adopted for labelling the welds identifies the flyer material ("A" for aluminium), the baseplate alloy ("CS" for carbon steel or "304" for stainless steel), and the collision point velocity ("H" for higher velocity and "L" for lower velocity). The welds produced with an interlayer are identified with an "I". So, A.304-L corresponds to a direct weld in which an aluminium flyer was projected on a stainless steel baseplate with a lower collision point velocity. In turn, the A.I.CS-H designates a weld made between an aluminium flyer and a carbon steel baseplate, using an interlayer and a higher collision point velocity.

The detonation velocity, which presents the same value as the collision point velocity in parallel welding, was measured following the procedure reported by Mendes et al. [23]. After welding, samples were collected longitudinally to the welding direction and prepared for metallographic analysis according to ASTM E3-11. The samples were observed in an optical microscope, Leica DM4000M LED. The microstructure of the welds was also studied by SEM, in a field emission scanning electron microscope, Zeiss Merlin VP Compact. This equipment, which was equipped with EDS, was used to study the chemical composition of the welds. The microstructural study was complemented by EBSD, which was conducted in a field emission scanning electron microscope, FEI Quanta 400FEG ESEM/EDAX Genesis X4M. The results obtained were analysed with the software OIM Analysis. The mechanical characterisation of the welds was conducted by nanoindentation and tensile-shear testing. The nanoindentation tests were performed by Micro Materials NanoTest equipment using a 30 mN load. The tensile-shear tests were conducted in quasi-static loading conditions (0.5 mm/min), using a 100 kN universal testing machine, Shimadzu AGS-X. The geometries of the tested specimens are based on Athar and Tolaminejad's work [24] and three samples were tested for each weld series.

Digital Image Correlation (DIC) by a GOM Aramis 5 M system was used to acquire the local strain fields of the tested specimens. The surface preparation of the specimens for the image acquirement was conducted according to Leitão et al. [25].

3. Results

3.1. Collision parameters and welding results

The impact velocity was computed for all weld series. For the conventional direct welding, the impact velocity was calculated using the equation presented by Kennedy [26] and reformulated by El-Sobky [27], relating the impact velocity, the explosive ratio and the Gurney velocity coefficient of the explosive mixture (Eq. (1)). The Gurney velocity was estimated through an empirical correlation with the detonation velocity obtained by Cooper [28] for ideal explosives: $\sqrt{2E} = V_d/2.97$. The limitations of this approach were discussed in detail by Carvalho et al. [29].

$$V_{p\,flyer} = \sqrt{2E}\left(\frac{3R^2}{R^2 + 5R + 4}\right)^{1/2} \tag{1}$$

R is the explosive ratio (dimensionless) and $\sqrt{2E}$ is the Gurney velocity coefficient of the explosive ($m{\cdot}s^{-1}$).

In order to calculate the impact velocity for the welds produced with an interlayer plate, a different approach must be used. After the collision between the flyer and the interlayer, these plates remain attached before colliding with the baseplate, and the impact velocity is the velocity of the flyer and the interlayer set. An approximate method to calculate the impact velocity consists of using the perfectly inelastic collision theory and the momentum conservation. So, the impact velocity of the final collision ($V_{pflyer+interl}$), was computed according to Eq. (2).

$$V_{p_{flyer+interl}} = \frac{m_{flyer}V_{p_{flyer}} + m_{interl.}V_{p_{interl.}}}{m_{flyer} + m_{interl.}}$$

$$\Longrightarrow V_{p_{flyer+interl}} = \frac{m_{flyer}V_{p_{flyer}}}{m_{flyer} + m_{interl.}} \tag{2}$$

$V_{pflyer+interl}$ is the impact velocity of the flyer and interlayer set, m_{flyer} is the mass of the flyer plate (kg), V_{pflyer} is the velocity of the flyer immediately before colliding with the interlayer ($m{\cdot}s^{-1}$), $m_{interl.}$ is the mass of the interlayer (kg).

Table 2 shows the collision point velocities measured, the impact velocities computed and the welding result for all the weld series. Among all the parameters tested, only the A.304-H series was unsuccessful, with the separation of the plates after the impact. In Table 2, the impact velocity values between parentheses would be the velocities obtained if no interlayer was used, which are similar to the values obtained by the direct welding with a similar collision point velocity. It shows that the use of the interlayer reduced the impact velocity by approximately 25%. This result is significant because it shows that this welding strategy allows a reduction in the impact velocity and in the energy lost in collision without changing the explosive ratio or the collision point velocity. Comparing the Al-SS series with high collision point velocities (A.304-H and A.I.304-H), the insertion of the interlayer allowed a good quality weld to be achieved.

Table 2
Values of collision point velocity, impact velocity and the welding result.

Weld series	V_c ($m{\cdot}s^{-1}$)	V_p ($m{\cdot}s^{-1}$)	Welding result
A.304-L	2300	703	Successful
A.I.304-L	1938	444 (592)	Successful
A.304-H	2836	523	Unsuccessful
A.I.304-H	2734	377 (504)	Successful
A.CS-L	1938	592	Successful
A.I.CS-L	1938	444 (592)	Successful
A.CS-H	2836	523	Successful
A.I.CS-H	2734	377 (504)	Successful

Table 3
Results of the tensile-shear tests and the fractographic analysis.

Weld series		Maximum load (kN)	Fracture region	Fracture mechanism
A.CS-L	Lowest	8.0	Interface	Ductile
	Highest	8.6	Outside the weld (flyer)	Ductile
A.CS-H	Lowest	6.9	Interface	Brittle
	Highest	7.5	Interface	Brittle
A.I.CS-L	Lowest	5.3	Interlayer	Ductile
	Highest	5.7	Interlayer	Ductile
A.I.CS-H	Lowest	4.3	Interlayer*	Ductile
	Highest	6.0	Interlayer	Ductile
A.304-L	Lowest	FDP	–	–
	Highest	FDP	–	–
A.304-H	Lowest	NT	–	–
	Highest	NT	–	–
A.I.304-L	Lowest	5.8	Interlayer	Ductile
	Highest	6.0	Interlayer	Ductile
A.I.304-H	Lowest	FDP	–	–
	Highest	4.7	Interlayer*	Ductile

FDP — specimen's failure during preparation.
NT — not tested due to weld failure.
* Fracture across the interlayer, with a small portion occurring at the interlayer/baseplate interface.

3.2. Weld mechanical behaviour

The results of the tensile-shear tests are shown in Table 3. As three specimens were tested per weld series, the table shows the lowest and the highest values of the maximum load registered for each series as well as the corresponding fracture region and mechanisms. The fractographic study of the welds is illustrated in Fig. 1.

Regarding the mechanical behaviour of the Al-CS welds, the table shows that the highest maximum load values were obtained for the weld series produced by direct impact welding (A.CS-L and A.CS-H). Among these series, better results were obtained for the welds produced with a lower collision point velocity, i.e. the A.CS-L welds. For most of the specimens of this series, the fracture occurred outside the weld region (on the AA6082 flyer), with a ductile behaviour (Fig. 1a). This indicates that the A.CS-L welding parameters provided good welding conditions. Although one of the specimens fractured at the flyer/baseplate interface (Fig. 1b), it presented a maximum load value that was very close to the others as well as a ductile fracture.

The A.CS-H welds fractured at the flyer/baseplate interface, with a brittle behaviour (Fig. 1c), resulting in a worse mechanical strength compared to the lower velocity direct weld (A.CS-L). However, the worst mechanical strength was presented by the welds produced with an interlayer (A.I.CS-L and A.I.CS-H), which fractured across the interlayer. The lower velocity specimens (A.I.CS-L) fractured exactly across the interlayer, with a ductile morphology (Fig. 1c). This resulted from the low strength of the interlayer material (AA1050), which was weaker than the similar and dissimilar bonding interfaces. The higher velocity specimens (A.I.CS-H) also fractured across the interlayer (with a similar mechanism to Fig. 1c), but one of the specimens presented a small portion of the fracture occurring at the interlayer/baseplate interface, resulting in the lowest maximum load of all the Al-CS series. The use of an interlayer for Al-CS joints did not result in an improvement of the weld's mechanical strength.

Regarding the Al-SS welding, Table 3 shows that the use of an interlayer had a positive effect on the mechanical behaviour of the welds. Better mechanical properties were obtained by welding with an interlayer, using either lower (A.304-L vs A.I.304-L) or higher (A.304-H vs

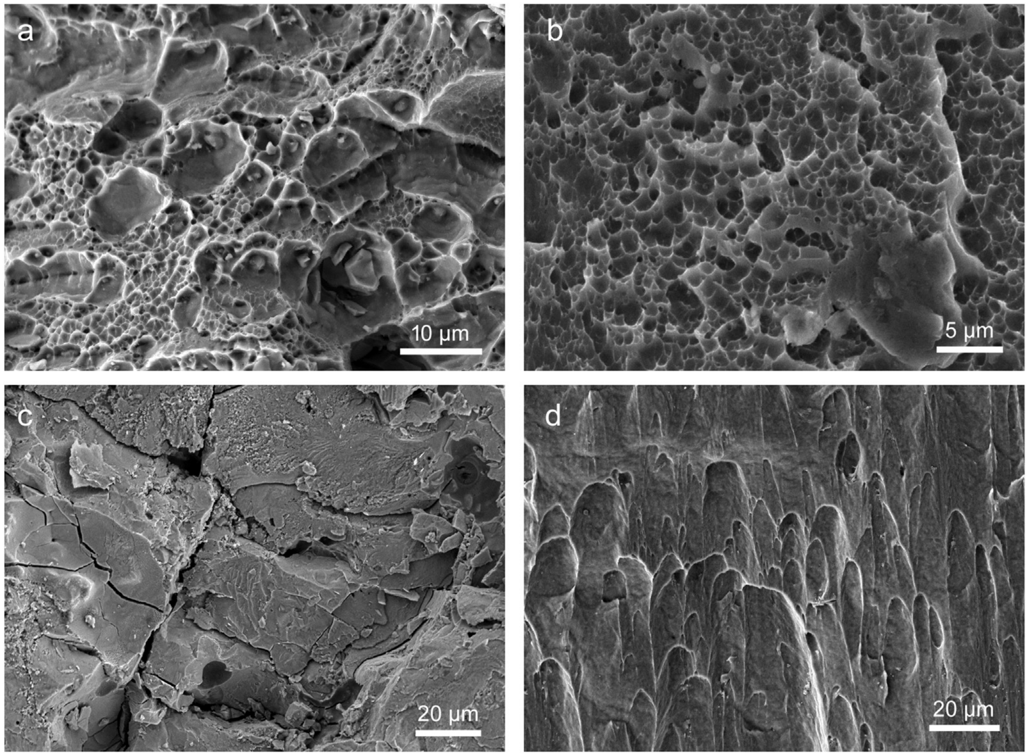

Fig. 1. Fracture surface micrographs of the Al-CS welds: (a) A.CS-L (ductile and outside the welding region), (b) A.CS-L (ductile at the interface), (c) A.CS-H (brittle at the interface) and (d) A.I.CS-L (ductile through the interlayer).

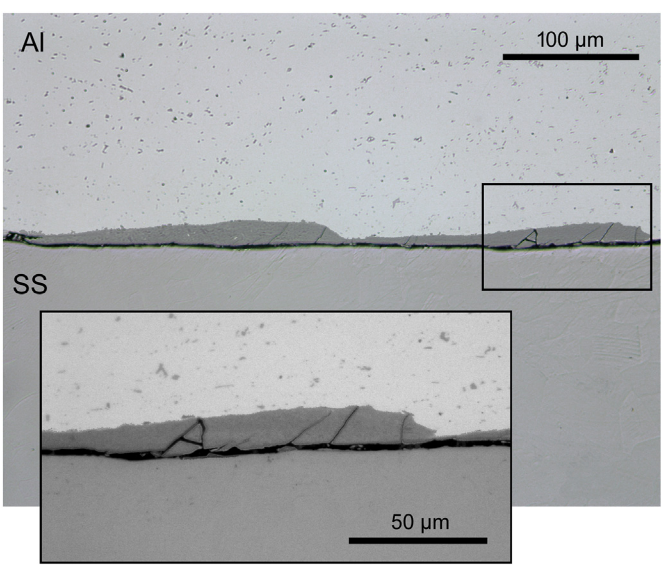

Fig. 2. Tensile-shear specimens from A.304-L weld that failed before testing with a crack propagating directly through the intermetallic layer.

A.I.304-H) detonation velocity explosive mixtures. In fact, for a higher collision point velocity, successful welding was only achieved with an interlayer. While the A.304-H series failed to weld the plates, the A.304-L series was consistent but cracked during the machining of the specimens. The separation during machining occurred by the propagation of a continuous and essentially rectilinear crack through the weld interface (Fig. 2). In agreement with that observed for Al-CS welding, the lower detonation velocity welds (A.I.304-L) presented the best mechanical behaviour, which fractured across the interlayer, with a ductile fracture. As reported for the Al-CS welds, the mechanical strength of the interlayered welds was also conditioned by the low strength of the interlayer material.

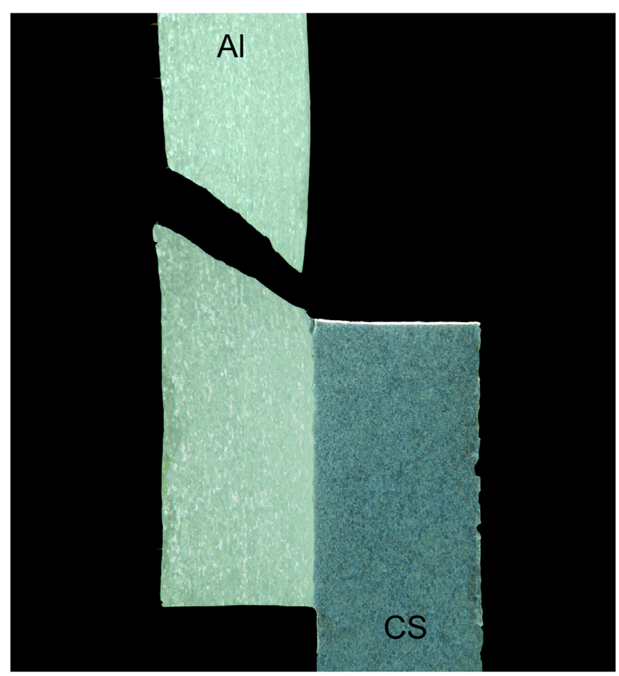

Fig. 3. Characteristic of the ductile fracture outside the welding region of A.CS-L weld.

Fig. 3 shows the longitudinal section of the specimens that fractured outside the weld region (A.CS-L). As reported above, the interface was able to withstand the testing stress, leading to a fracture in the aluminium flyer. In turn, to characterise all the fracture types occurring at the weld interface, Fig. 4 shows the strain distribution maps acquired by DIC. The equivalent Von Mises strain at the maximum load is also

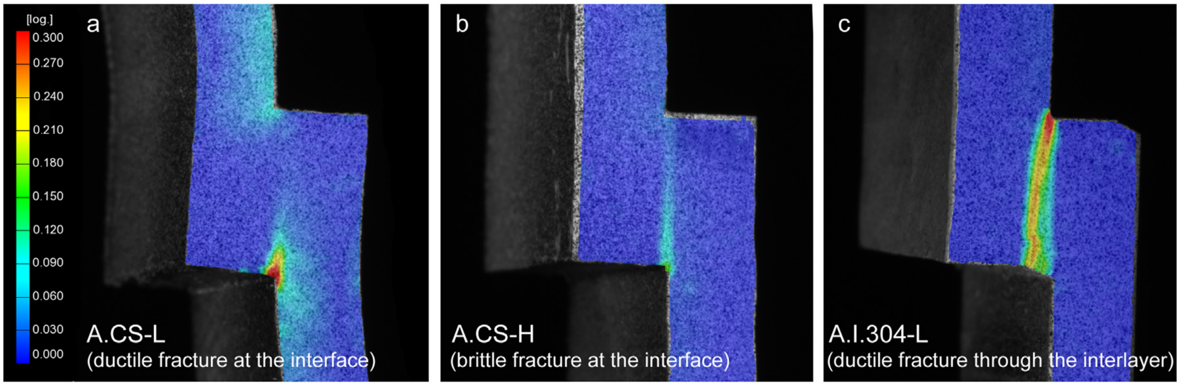

Fig. 4. DIC by GOM Aramis of each interfacial fracture: (a) A.CS-L (ductile at the interface), (b) A.CS-H (brittle at the interface) and (c) A.I.CS-L (ductile through the interlayer).

illustrated in the figure. A.CS-L (Fig. 4a) and A.I.304-L (Fig. 4c) presented more deformation, which agrees well with the ductile behaviour of the fractures, while A.CS-H (Fig. 4b) presented less deformation and a brittle fracture. The interlayered weld presented the most intense deformation because of the low strength and high ductility of the AA1050 interlayer alloy, where the fracture took place.

Table 4 shows the results of EDS analyses conducted on each of the fracture surfaces displayed in Fig. 1. The chemical composition of the fracture surfaces corresponding to the fracture outside the welding region in the flyer plate (Fig. 1a) and the ductile fracture at the interface (Fig. 1b) matches the chemical composition of AA6082 well. In turn, both Al and Fe were detected in the fracture surfaces, associated with brittle fracture at the interface (Fig. 1c). The fracture surface across the interlayer (Fig. 1d), presented a pure aluminium composition, associated with the AA1050 composition.

3.3. Weld interface analysis

After obtaining the mechanical strength and behaviour under tensile-shear solicitation of the weld series, it is essential to perceive the microstructural characteristics that led to each mechanical behaviour. Fig. 5 shows the interface morphology of all the Al-SS welds. As reported in Section 3.1, a consistent weld was obtained by direct welding only by using a low collision point velocity (Fig. 5a). Using an interlayer, the welding was successful for both low and high collision point velocities, as shown in Fig. 5c and d, respectively. Fig. 6 presents the interface morphology of the Al-CS welds. No welding failure occurred for both direct and interlayered welding. In Figs. 5 and 6 different morphologies can be observed among the different configurations, parameters and alloys.

The first feature to be analysed is the welding failure of the A.304-H weld (Fig. 5b). The use of a high collision point velocity together with a high impact velocity led to excessive interfacial energy, which resulted in excessive melting and prevented successful bonding. However, adding an intermediate plate (Fig. 5d), which led to a 25% decrease in the impact velocity (and the energy lost in collision) for similar detonation/collision point velocities, the weld was achieved.

The distinct morphologies found can be evaluated from several points of views since they are related to the collision point velocity, the explosive ratio, the interlayer and the properties of the welded alloys. Each one of these parameters affects the interface in different ways. The collision point velocity is usually related to melting on the interface and jet entrapment [30]. The alloys' properties affect the phenomena occurring at the interface since the difference in properties between the flyer and baseplate is one of the features that dictates the possibility of wave formation [29]. The explosive ratio, among other features, influences the interfacial shapes just like the wavelength and amplitude [31].

For both Al-CS and Al-SS combinations, there are considerable differences in the morphology of the Al/Al interface (flyer/interlayer) between the lower and higher collision point velocities. This difference is possibly related to the explosive ratio and impact velocity. The interlayered welds conducted with ANFO (ratio of 2.5) in Figs. 5c and 6c presented much bigger waves than the welds conducted with E + EPS (ratio of 1), in Figs. 5d and 6d. A similar characteristic was found at the dissimilar interface for the Al-CS joints without an interlayer, i.e. the welds produced using a higher explosive ratio (Fig. 6a) presented much bigger waves than the samples produced with a lower ratio (Fig. 6b). The Al-SS interface did not form waves regardless of the parameters.

The microstructural differences resulting from using different baseplate alloys become evident from the level of deformation and the presence of waves. While the carbon steel baseplate presented large waves with a substantial plastic deformation (Fig. 6a and c), the stainless steel baseplate did not present wave formation (Fig. 5a and c). However, it should be noted that, for a higher collision point velocity (Fig. 5d), the stainless steel baseplate presents more irregularities at the weld interface, which possibly indicates a very initial stage of wave formation.

The mechanical tests showed that the best results achieved for direct and interlayered welding were the experiments with low collision point velocities: A.304-L and A.I.304-L (Al-SS) and A.CS-L and A.I.CS-L (Al-CS). An in-depth microstructural study of these welds was conducted to understand the reasons underlying their improved mechanical strength. EBSD analysis with Inverse Pole Figure (IPF) was used to identify the deformation and recrystallisation characteristics of these four welds. Fig. 7 shows the images for the Al-SS welds. There is no significant difference between the A.304-L direct weld (Fig. 7a) and the A.I.304-L interlayered weld (Fig. 7b) in terms of strain distribution or recrystallisation. The difference in mechanical behaviour between these two series comes from the difference in the impact velocity and energy lost in collision, which is slightly excessive in direct welding. This resulted in a thicker interfacial layer (arrow) for the A.304-L direct weld (Fig. 7a) that was fully continuous throughout the interface and consequently led to poor mechanical behaviour compared to the weld with an interlayer, A.I.304-L. The cracks on these layers indicate a brittle nature.

On the other hand, the Al-CS welds with the best mechanical

Table 4
Chemical composition (atomic %) of the fracture surfaces.

Surface	Al	Mg	Si	Fe
Fig. 1a	96.7	1.6	1.7	–
Fig. 1b	99.0	1.0	–	–
Fig. 1c	80.9	–	–	19.1
Fig. 1d	100	–	–	–

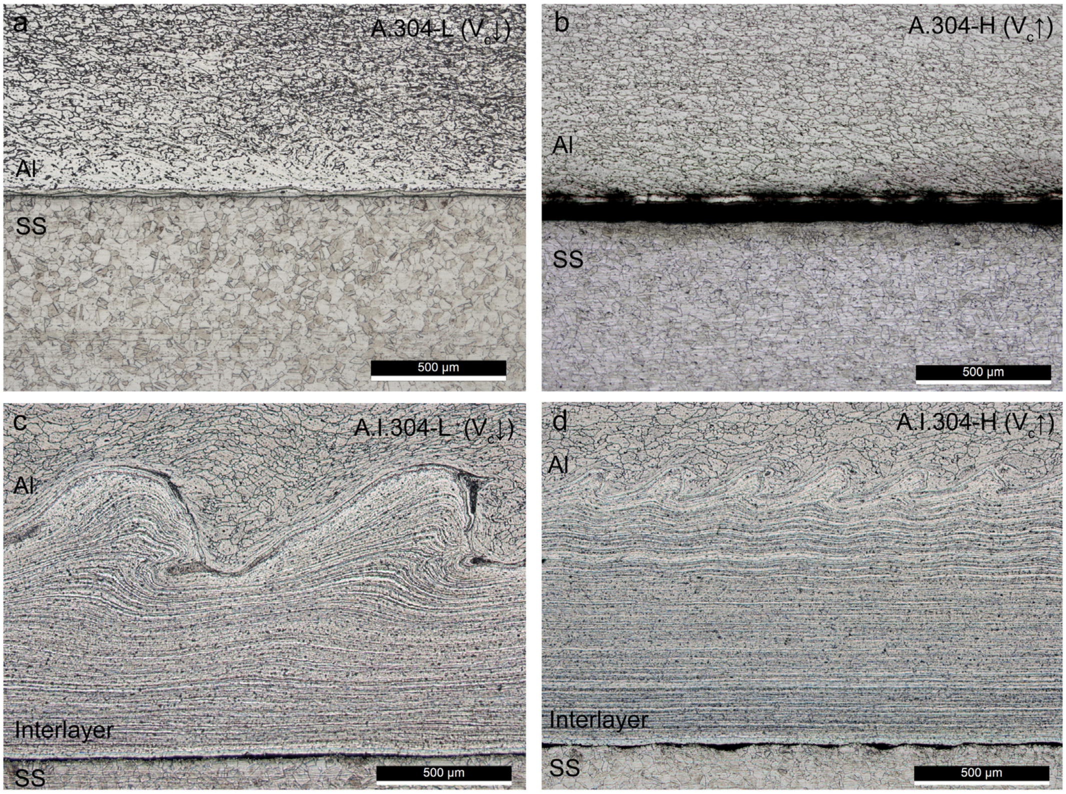

Fig. 5. Morphology of the interface of the Al-SS welds: (a) A.304-L, (b) A.304-H, (c) A.I.304-L and (d) A.I.304-H.

strength (A.CS-L and A.I.CS-L), presented a high strain level and similar interfacial distribution. Both welds presented curled waves with a coiled shape formed from the steel, that rolled over themselves encompassing the interfacial phases with strongly-deformed grains (Fig. 8a and b). The intertwined wave shape facilitates the bonding of the plates and locks them together, leading to an excellent mechanical

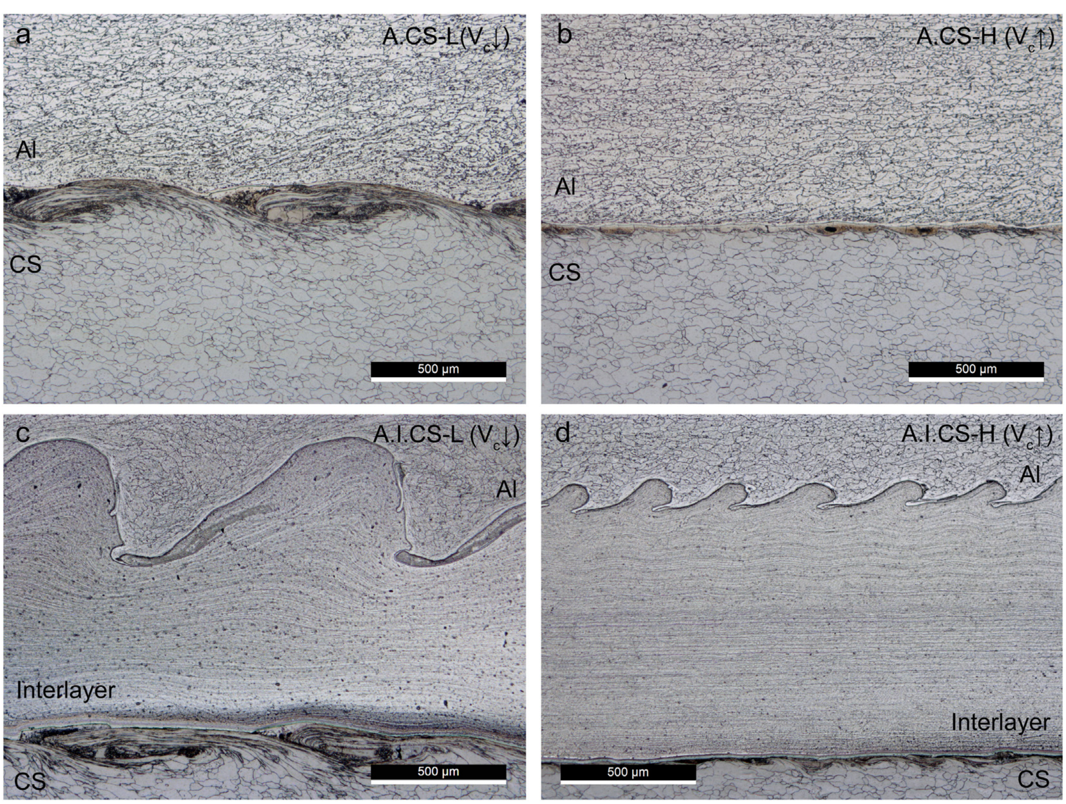

Fig. 6. Morphology of the interface of the Al-CS welds: (a) A.CS-L, (b) A.CS-H, (c) A.I.CS-L and (d) A.I.CS-H.

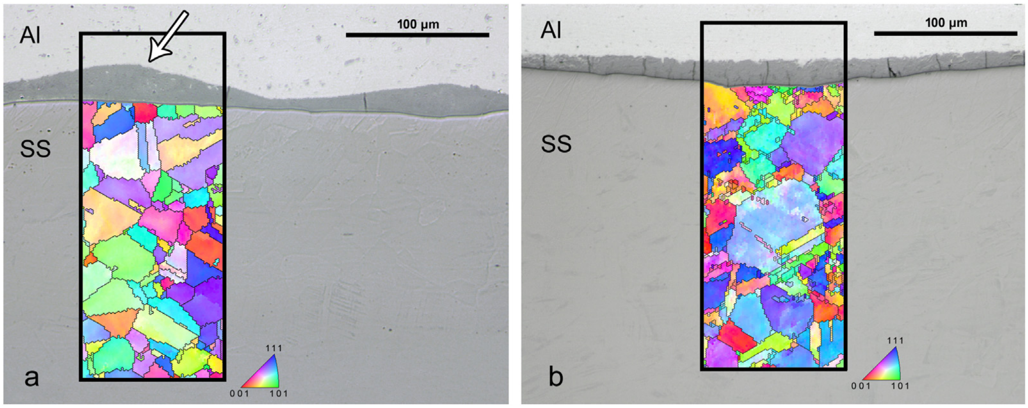

Fig. 7. EBSD analysis by IFP of the Al-SS welds: (a) A.304-L and (b) A.I.304-L.

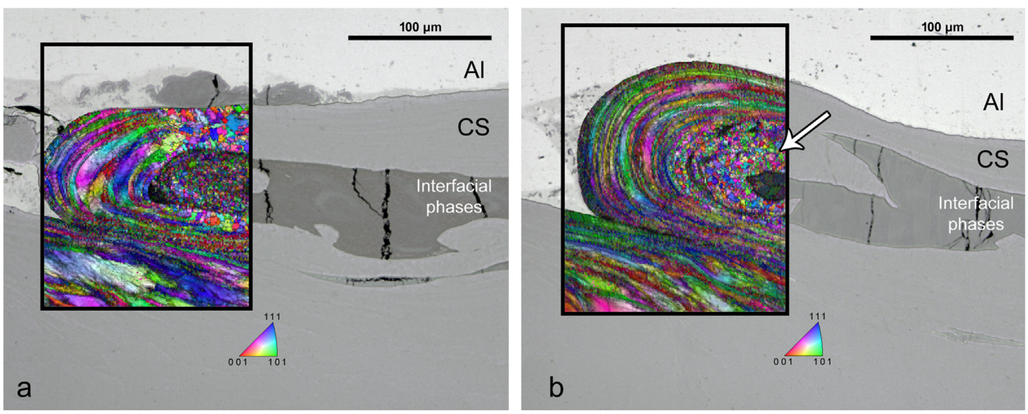

Fig. 8. EBSD analysis by IFP of the Al-CS welds: (a) A.CS-L and (b) A.I.CS-L.

behaviour for both welds. Fig. 8b also shows the presence of a recrystallisation region within the wave (arrow), which is related to the extreme conditions of temperature and strain occurring inside the vortex. The difference in mechanical strength between these two welds was dictated not by differences in microstructure or interfacial morphology, but by the presence of the AA1050 interlayer that has a lower strength compared to the flyer and baseplate materials.

Comparing the Al-SS and Al-CS welds, the stronger bonding achieved by the Al-CS welds agrees well with the higher levels of interfacial deformation. For the Al-CS welds, the base material deformed in a curled shape while the Al-SS welds did not present a significant deformation that could bond the materials and interrupt the continuity of the interfacial layer.

Figs. 9 and 10 show the SEM analysis for the Al-SS and Al-CS welds, respectively. Table 5 shows the EDS chemical composition results. Analysing the results for the Al-SS welds, both series presented a continuous interfacial layer, which was thicker for the direct weld than for the interlayered weld. The chemical compositions (regions 1 to 4 in Table 5) consist mainly of Al and Fe (with the presence of Cr, Ni, Si and Mg). Extremely high nano-hardness values, ranging between 4.7 and 12.4 GPa, were also measured in these zones (Fig. 11a and b). The brittle nature, the nano-hardness and the mixed composition match the properties of intermetallic phases. The relative quantity of Al and Fe in the intermetallic layer varied according to the zone under analysis. The EDS analyses show that for the direct welding (Fig. 9c), there is a lower presence of Fe than in the interlayered welding (Fig. 9d). The morphology inside these interfacial layers is also quite different, becoming more complex with an increase in the participation of iron (Fig. 9c and d).

Fig. 10 shows that the interface morphologies of the Al-CS welds are quite similar. Despite having the same baseplate, the interfacial alloy in contact to the steel is different (AA6082 flyer or AA1050 interlayer), and therefore, the chemical compositions of regions 5 to 8 presented a slight difference regarding the Si and Mg which are present in the AA6082 direct weld. Table 5 shows that both interfacial layers presented a mixed Al—Fe composition and an extremely high nano-hardness, ranging between 3.9 and 12.8 GPa (Fig. 11c and d), which confirms that it is also a brittle intermetallic material.

The Al-CS welds presented more heterogeneous compositions in which, depending on the location within the intermetallic layer, the composition is Al-richer or Fe-richer. The intermetallic morphology of both the direct and interlayered welds is similar, with some dendrites indicating melting in these regions. Compared to the Al-SS welds, the composition in these zones is simpler, essentially composed of iron and aluminium with an increased participation of iron.

Paul et al. [32] discussed the complexity of the definition and characterisation of an entire intermetallic region of explosive welded samples. The extreme characteristics of this process result in transformations that are far from equilibrium and favour the formation of metastable intermetallic phases [33,34] and hinder an accurate identification of all the different intermetallic phases that may be present within an entire intermetallic layer in an explosion joint. Carvalho et al. [1] identified Fe_4Al_{13} and Fe_2Al_5 at the interface of dissimilar aluminium and carbon steel welds. The formation of these phases in the intermetallic volumes of the present Al-CS welds is likely. Regarding the Al-SS welds, the range of possible phases is even higher, considering the significant presence of alloying elements in the stainless steel that could form more complex intermetallic phases. However, rather than identifying each phase within the intermetallic layer, what is important in explosive welding is to understand how the intermetallics are distributed at the weld interface and their effect on the mechanical properties of the joint.

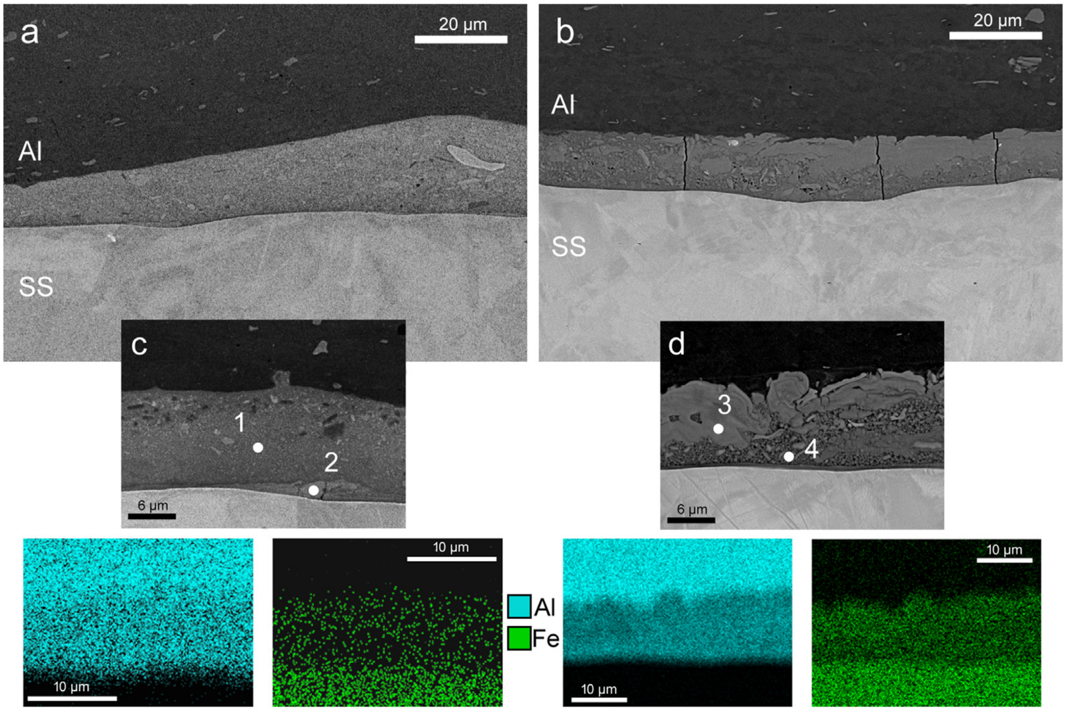

Fig. 9. SEM analysis of the Al-SS welds and EDS locations: (a) A.304-L and (b) A.I.304-L.

4. Discussion

Analysing the mechanical performance and the welding results, it is clear that the Al-SS combination presents a worse weldability than Al-CS. In fact, the Al-SS weld benefits from the use of the interlayer plate because it widens the range of possible parameters. The energy loss caused by the intermediate collision of the flyer plate with the interlayer allowed consistent Al-SS welds even for high detonation velocities. Without the interlayer, the difference in physical properties between the flyer and the baseplate prevented the achievement of good quality welds, and even the consistent welds failed during the preparation of the tensile-shear specimens. Moreover, although some authors [12,35] have proved the collision point velocity limitations for aluminium-flyer welds, the impact velocity also has a significant influence on the achievement of consistent welds. This is proved by the Al-SS interlayered welding with a higher collision point velocity (A.I.304-H) in which the lower impact velocity made the weld possible.

Regarding the intermetallic distribution and composition, there is a

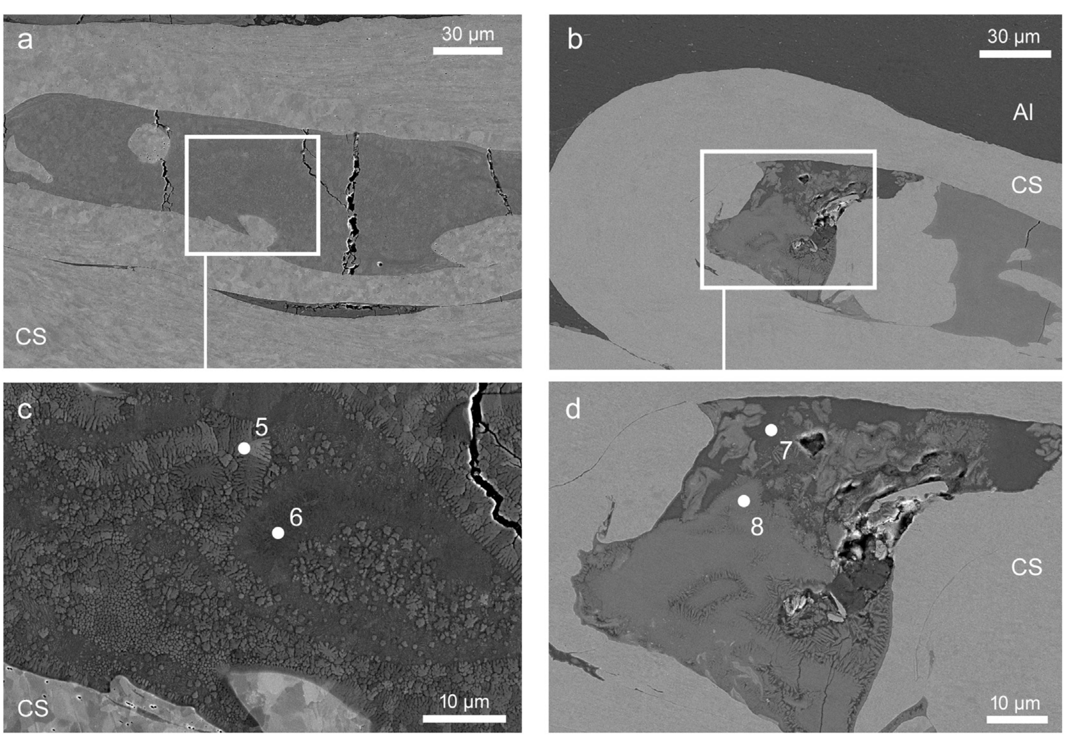

Fig. 10. SEM analysis of the Al-CS welds and EDS locations: (a) A.CS-L and (b) A.I.CS-L.

Table 5
Chemical composition (atomic %) of the intermetallic material.

Region	Al	Fe	Cr	Ni	Si	Mg
1	88.5	7.2	2.0	1.0	0.6	0.7
2	86.9	10.1	3.0	–	–	–
3	74.4	18.7	5.2	1.8	–	–
4	82.4	12.7	3.5	1.3	0.1	–
5	47.8	51.6	–	–	0.5	0.1
6	59.6	39.3	–	–	0.5	0.6
7	92.3	7.7	–	–	–	–
8	78.7	21.3	–	–	–	–

very close relation between the interface morphology and microstructure, and the formation and distribution of the intermetallic phases. While there was no wavy formation on the Al-SS welds, big curled waves were formed on the Al-CS welds, indicating a strong relative movement between the materials at the interface. In fact, despite having the same flyer plate and the same welding parameters, the dissimilarity of the properties between carbon steel and stainless steel (especially thermal conductivity and hardness) led to extremely contrasting morphologies, especially for low collision point velocities. This shows that the parameter requirements for wave formation (process velocities and ratio) on the stainless steel are higher than for the carbon steel. The differences in properties between stainless steel and aluminium usually make it very difficult to achieve these high requirements and lead to welding failure [12].

The intertwining of the alloys in Al-CS welding leads to a more significant mixing of the elements when comparing the two alloy combinations. Nevertheless, despite a stronger mixing and interaction, the curled waves' microstructure, circling and interrupting what would have been a continuous intermetallic layer, led to a much stronger anchorage and metallurgical bonding. These characteristics were evidenced during the tensile-shear tests, where the Al-CS welds presented the best mechanical strength. Fig. 12 shows this phenomenon in detail. There is no location where a fracture could propagate only through the brittle intermetallic material. These curled waves with a coiled shape are reported in several works, and they are usually achieved in explosive welding of materials with notable density differences such as Al-CS in this work and in [36], Al–Cu [24,37,38], Ta–Cu [39,40], Ta-SS [41] and Ti–Fe [42,43]. In all these works, the wave is formed by the material with the highest density.

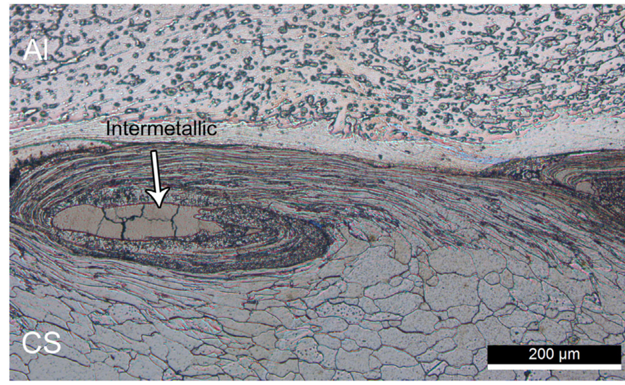

Fig. 12. Interfacial morphology of the A.CS-L weld. Coiled shape curled waves surrounding the intermetallic material.

On the other hand, the Al-SS interface with the presence of a continuous intermetallic layer was harmful to the mechanical properties. This is clear from analysing the machined tensile-shear samples in Fig. 2, where there is a continuous crack throughout the interface that led to the separation of plates. Also, welding 304 stainless steel leads to the presence of alloy elements (like chromium and nickel) that will form more complex brittle intermetallic phases with iron. As a result, a continuous, brittle intermetallic layer with diverse intermetallic phases is formed. The flat morphology of the interface does not facilitate the anchoring of the welded materials in a way that could neutralise the brittleness and the harmful effects of the intermetallic phases.

In explosive welding, it is becoming clear that only the presence and quantity of intermetallics is not enough to explain the quality and strength of a weld joint. The results show that it is essential to understand how the intermetallics interact with the stress mechanisms that will act at the joint. Indeed, the intermetallic phases in dissimilar welding are often very hard and brittle, and therefore, harmful to the mechanical properties. However, specifically in explosive welding, where bulk melting is not present, the intermetallic formation is also a sign of metallurgical interaction and has been reported by several authors [12,44] as being present in most of the good quality joints. When welding alloys that easily form intermetallic phases (like Al–Cu, Al–Fe and Al–Ni), the absence of intermetallic formation usually suggests a lack of interaction and insufficient energy applied since the

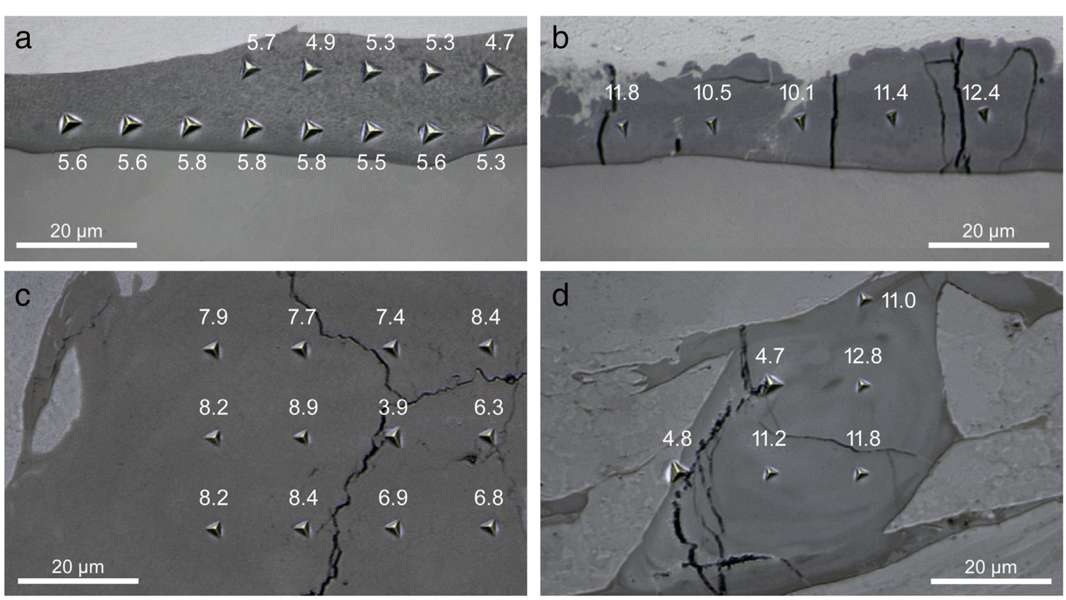

Fig. 11. Nano-hardness values (GPa) measured in the intermetallic material of the welds: (a) A.304-L, (b) A.I.304-L, (c) A.CS-L and (d) A.I.CS-L.

intermetallic formation is almost inevitable for these combinations. Therefore, the main characteristic to seek in the explosive welding of dissimilar materials is not the complete absence of intermetallic formations, but to perceive how the intermetallics are inserted in the joint in terms of distribution, shape and morphology. It is necessary to achieve an appropriate metallurgical interaction, avoid thick and completely continuous layers, and obtain interfacial morphologies that can accommodate deformation and stresses, avoiding these being directed precisely on the intermetallics.

5. Conclusions

The influence of interlayered welding on the microstructure and the mechanical behaviour of aluminium-carbon steel and aluminium-stainless steel clads produced by explosive welding was studied in this research. Different series of welds were produced with and without an interlayer, testing different welding parameters. The morphology and the microstructure of the weld interface were evaluated as well as their effects on the mechanical behaviour of the welds. The following conclusions can be reached:

- The combination of aluminium to carbon steel has a better weldability than aluminium to stainless steel. For both combinations, the low collision point velocity experiments were always better in terms of microstructure and mechanical performance.
- The use of the aluminium interlayer improved the weldability and the mechanical performance of aluminium to stainless steel welds, although the weld's mechanical strength was restricted by the low strength of the interlayer. On the other hand, it had no beneficial effect on the mechanical properties of the aluminium to carbon steel welds. An aluminium to carbon steel joint with excellent tensile-shear properties was achieved by low-velocity direct welding, with the fracture occurring outside the joining region.
- The presence of hard and brittle intermetallics by itself does not indicate a poor-quality explosive weld. The way that the interface accommodates and distributes the intermetallic dictates the weld quality. Weld interfaces with morphologies that can prevent the intermetallics from being regions favourable to an uninterrupted propagation of a brittle fracture through the interface present the best mechanical behaviour.

Data availability

The raw/processed data required to reproduce these findings cannot be shared at this time as the data also forms part of an ongoing study.

Acknowledgements

This research is sponsored by FEDER funds through the programme COMPETE – *Programa Operacional Factores de Competitividade* – and by national funds through FCT – *Fundação para a Ciência e a Tecnologia*, under the project UID/EMS/00285/2013. The first author, G.H.S.F.L. Carvalho, is supported by the *Conselho Nacional de Desenvolvimento Científico e Tecnológico* (CNPq) from Brazil.

References

[1] G.H.S.F.L. Carvalho, I. Galvão, R. Mendes, R.M. Leal, A. Loureiro, Formation of intermetallic structures at the interface of steel-to-aluminium explosive welds, Mater. Charact. 142 (2018) 432–442, https://doi.org/10.1016/j.matchar.2018.06.005.

[2] H. Geng, L. Sun, G. Li, J. Cui, L. Huang, Z. Xu, Fatigue fracture properties of magnetic pulse welded dissimilar Al-Fe lap joints, Int. J. Fatigue 121 (2019) 146–154, https://doi.org/10.1016/j.ijfatigue.2018.12.027.

[3] S. Su, S. Chen, Y. Mao, J. Xiao, A. Vivek, G. Daehn, Joining aluminium alloy 5A06 to stainless steel 321 by vaporizing foil actuators welding with an interlayer, Metals (Basel) 9 (2019) 43, https://doi.org/10.3390/met9010043.

[4] X. Wang, F. Li, T. Huang, X. Wang, H. Liu, Experimental and numerical study on the laser shock welding of aluminum to stainless steel, Opt. Lasers Eng. 115 (2019) 74–85, https://doi.org/10.1016/j.optlaseng.2018.11.012.

[5] H. Wang, Y. Wang, High-velocity impact welding process: a review, Metals (Basel) 9 (2019) 144, https://doi.org/10.3390/met9020144.

[6] Y. Kaya, Microstructural, mechanical and corrosion investigations of ship steel-aluminum bimetal composites produced by explosive welding, Metals (Basel) 8 (2018) 544, https://doi.org/10.3390/met8070544.

[7] L. Tricarico, R. Spina, D. Sorgente, M. Brandizzi, Effects of heat treatments on mechanical properties of Fe/Al explosion-welded structural transition joints, Mater. Des. 30 (2009) 2693–2700, https://doi.org/10.1016/j.matdes.2008.10.010.

[8] P. Corigliano, V. Crupi, E. Guglielmino, Non linear finite element simulation of explosive welded joints of dissimilar metals for shipbuilding applications, Ocean Eng. 160 (2018) 346–353, https://doi.org/10.1016/j.oceaneng.2018.04.070.

[9] A. Gullino, P. Matteis, F. D'Aiuto, Review of aluminum-to-steel welding technologies for car-body applications, Metals (Basel) 9 (2019) 315, https://doi.org/10.3390/met9030315.

[10] X. Guo, H. Wang, Z. Liu, L. Wang, F. Ma, J. Tao, Interface and performance of CLAM steel/aluminum clad tube prepared by explosive bonding method, Int. J. Adv. Manuf. Technol. 82 (2016) 543–548, https://doi.org/10.1007/s00170-015-7380-z.

[11] P. Corigliano, V. Crupi, E. Guglielmino, A. Mariano Sili, Full-field analysis of AL/FE explosive welded joints for shipbuilding applications, Mar. Struct. 57 (2018) 207–218, https://doi.org/10.1016/j.marstruc.2017.10.004.

[12] G.H.S.F.L. Carvalho, I. Galvão, R. Mendes, R.M. Leal, A. Loureiro, Explosive welding of aluminium to stainless steel, J. Mater. Process. Technol. 262 (2018) 340–349, https://doi.org/10.1016/j.jmatprotec.2018.06.042.

[13] S. Saravanan, K. Raghukandan, Influence of interlayer in explosive cladding of dissimilar metals, Mater. Manuf. Process. 28 (2013) 589–594, https://doi.org/10.1080/10426914.2012.736665.

[14] P. Manikandan, K. Hokamoto, M. Fujita, K. Raghukandan, R. Tomoshige, Control of energetic conditions by employing interlayer of different thickness for explosive welding of titanium/304 stainless steel, J. Mater. Process. Technol. 195 (2008) 232–240, https://doi.org/10.1016/j.jmatprotec.2007.05.002.

[15] D.V. Lazurenko, I.A. Bataev, V.I. Mali, E.A. Lozhkina, M.A. Esikov, V.A. Bataev, Structural transformations occurring upon explosive welding of alloy steel and high-strength titanium, Phys. Met. Metallogr. 119 (2018) 469–476, https://doi.org/10.1134/S0031918X18050095.

[16] M.A. Habib, H. Keno, R. Uchida, A. Mori, K. Hokamoto, Cladding of titanium and magnesium alloy plates using energy-controlled underwater three layer explosive welding, J. Mater. Process. Technol. 217 (2015) 310–316, https://doi.org/10.1016/j.jmatprotec.2014.11.032.

[17] P. Bazarnik, B. Adamczyk-Cieślak, A. Gałka, B. Płonka, L. Snieżek, M. Cantoni, M. Lewandowska, Mechanical and microstructural characteristics of Ti6Al4V/AA2519 and Ti6Al4V/AA1050/AA2519 laminates manufactured by explosive welding, Mater. Des. 111 (2016) 146–157, https://doi.org/10.1016/j.matdes.2016.08.088.

[18] S. Saravanan, K. Raghukandan, K. Hokamoto, Improved microstructure and mechanical properties of dissimilar explosive cladding by means of interlayer technique, Arch. Civ. Mech. Eng. 16 (2016) 563–568, https://doi.org/10.1016/j.acme.2016.03.009.

[19] K. Hokamoto, T. Izuma, M. Fujita, New explosive welding technique to weld aluminum alloy and stainless steel plates using a stainless steel intermediate plate, Metall. Trans. A 24 (1993) 2289–2297, https://doi.org/10.1007/BF02648602.

[20] J.H. Han, J.P. Ahn, M.C. Shin, Effect of interlayer thickness on shear deformation behavior of AA5083 aluminum alloy/SS41 steel plates manufactured by explosive welding, J. Mater. Sci. 38 (2003) 13–18, https://doi.org/10.1023/A:1021197328946.

[21] S.M. Aceves, F. Espinosa-Loza, J.W. Elmer, R. Huber, Comparison of Cu, Ti and Ta interlayer explosively fabricated aluminum to stainless steel transition joints for cryogenic pressurized hydrogen storage, Int. J. Hydrog. Energy 40 (2015) 1490–1503, https://doi.org/10.1016/j.ijhydene.2014.11.038.

[22] R. Mendes, J. Ribeiro, I. Plaksin, J. Campos, B. Tavares, Differences between the detonation behavior of emulsion explosives sensitized with glass or with polymeric micro-balloons, J. Phys. Conf. Ser. 500 (2014) 1–6, https://doi.org/10.1088/1742-6596/500/5/052030.

[23] R. Mendes, J.B. Ribeiro, A. Loureiro, Effect of explosive characteristics on the explosive welding of stainless steel to carbon steel in cylindrical configuration, Mater. Des. 51 (2013) 182–192, https://doi.org/10.1016/j.matdes.2013.03.069.

[24] M.M. Hoseini Athar, B. Tolaminejad, Weldability window and the effect of interface morphology on the properties of Al/Cu/Al laminated composites fabricated by explosive welding, Mater. Des. 86 (2015) 516–525, https://doi.org/10.1016/j.matdes.2015.07.114.

[25] C. Leitão, I. Galvão, R.M. Leal, D.M. Rodrigues, Determination of local constitutive properties of aluminium friction stir welds using digital image correlation, Mater. Des. 33 (2012) 69–74, https://doi.org/10.1016/j.matdes.2011.07.009.

[26] J.E. Kennedy, Gurney Energy of Explosives: Estimation of the Velocity and Impulse Imparted to Driven Metal, Sandia Laboratories, New Mexico, USA, 1970.

[27] H. El-Sobky, Mechanics of explosive welding, in: T.Z. Blazynski (Ed.), Explos. Welding, Form. Compact, Springer Netherlands, Dordrecht, 1983, pp. 189–217, , https://doi.org/10.1007/978-94-011-9751-9_6.

[28] P.W. Cooper, Explosive Engineering, Wiley-VCH, New York, USA, 1996.

[29] G.H.S.F.L. Carvalho, R. Mendes, R.M. Leal, I. Galvão, A. Loureiro, Effect of the flyer material on the interface phenomena in aluminium and copper explosive welds, Mater. Des. 122 (2017) 172–183, https://doi.org/10.1016/j.matdes.2017.02.087.

[30] G.R. Cowan, A.H. Holtzman, Flow configurations in colliding plates: explosive bonding, J. Appl. Phys. 34 (1963) 928–939, https://doi.org/10.1063/1.1729565.

[31] A. Durgutlu, B. Gülenç, F. Findik, Examination of copper/stainless steel joints

formed by explosive welding, Mater. Des. 26 (2005) 497–507, https://doi.org/10.1016/j.matdes.2004.07.021.

[32] H. Paul, L. Lityńska-Dobrzyńska, M. Prazmowski, Microstructure and phase constitution near the interface of explosively welded aluminum/copper plates, Metall. Mater. Trans. A 44 (2013) 3836–3851, https://doi.org/10.1007/s11661-013-1703-1.

[33] I.A. Bataev, D.V. Lazurenko, S. Tanaka, K. Hokamoto, A.A. Bataev, Y. Guo, A.M. Jorge, High cooling rates and metastable phases at the interfaces of explosively welded materials, Acta Mater. 135 (2017) 277–289, https://doi.org/10.1016/j.actamat.2017.06.038.

[34] I.A. Bataev, T.S. Ogneva, A.A. Bataev, V.I. Mali, M.A. Esikov, D.V. Lazurenko, Y. Guo, A.M. Jorge Junior, Explosively welded multilayer Ni-Al composites, Mater. Des. 88 (2015) 1082–1087, https://doi.org/10.1016/j.matdes.2015.09.103.

[35] G.H.S.F.L. Carvalho, I. Galvão, R. Mendes, R.M. Leal, A. Loureiro, Weldability of aluminium-copper in explosive welding, Int. J. Adv. Manuf. Technol. (2019), https://doi.org/10.1007/s00170-019-03841-9.

[36] A. Szecket, O.T. Inal, D.J. Vigueras, J. Rocco, A wavy versus straight interface in the explosive welding of aluminum to steel, J. Vac. Sci. Technol. A 3 (1985) 2588–2593, https://doi.org/10.1116/1.572839.

[37] G.H.S.F.L. Carvalho, I. Galvão, R. Mendes, R.M. Leal, A. Loureiro, Influence of base material properties on copper and aluminium–copper explosive welds, Sci. Technol. Weld. Join. 23 (2018) 501–507, https://doi.org/10.1080/13621718.2017.1417783.

[38] Y. Wei, H. Li, F. Sun, J. Zou, The interfacial characterization and performance of Cu/Al-conductive heads processed by explosion welding, cold pressure welding, and solid-liquid casting, Metals (Basel) 9 (2019) 237, https://doi.org/10.3390/met9020237.

[39] P. Parchuri, S. Kotegawa, H. Yamamoto, K. Ito, A. Mori, K. Hokamoto, Benefits of intermediate-layer formation at the interface of Nb/Cu and Ta/Cu explosive clads, Mater. Des. 166 (2019) 107610, , https://doi.org/10.1016/j.matdes.2019.107610.

[40] B.A. Greenberg, M.A. Ivanov, V.V. Rybin, O.A. Elkina, O.V. Antonova, A.M. Patselov, A.V. Inozemtsev, A.V. Plotnikov, A.Y. Volkova, Y.P. Besshaposhnikov, The problem of intermixing of metals possessing no mutual solubility upon explosion welding (Cu–Ta, Fe–Ag, Al–Ta), Mater. Charact. 75 (2013) 51–62, https://doi.org/10.1016/j.matchar.2012.10.011.

[41] H. Paul, M.M. Miszczyk, R. Chulist, M. Prażmowski, J. Morgiel, A. Gałka, M. Faryna, F. Brisset, Microstructure and phase constitution in the bonding zone of explosively welded tantalum and stainless steel sheets, Mater. Des. 153 (2018) 177–189, https://doi.org/10.1016/j.matdes.2018.05.014.

[42] Q. Chu, M. Zhang, J. Li, C. Yan, Experimental and numerical investigation of microstructure and mechanical behavior of titanium/steel interfaces prepared by explosive welding, Mater. Sci. Eng. A 689 (2017) 323–331, https://doi.org/10.1016/j.msea.2017.02.075.

[43] M. Gloc, M. Wachowski, T. Plocinski, K.J. Kurzydlowski, Microstructural and microanalysis investigations of bond titanium grade1/low alloy steel st52-3N obtained by explosive welding, J. Alloys Compd. 671 (2016) 446–451, https://doi.org/10.1016/j.jallcom.2016.02.120.

[44] D.M. Fronczek, R. Chulist, L. Litynska-Dobrzynska, S. Kac, N. Schell, Z. Kania, Z. Szulc, J. Wojewoda-Budka, Microstructure and kinetics of intermetallic phase growth of three-layered A1050/AZ31/A1050 clads prepared by explosive welding combined with subsequent annealing, Mater. Des. 130 (2017) 120–130, https://doi.org/10.1016/j.matdes.2017.05.051.